CHEMISTRY
A EUROPEAN JOURNAL

FULL PAPER

DOI: 10.1002/chem.201202105

Central-Atom Size Effects on the Methyl Torsions of Group XIV Tetratolyls

Maggie C. C. Ng,[a] Jason B. Harper,[a] Anton P. J. Stampfl,[b] Gordon J. Kearley,[b] Stéphane Rols,[c] and John A. Stride*[a, b]

Abstract: The Group XIV tetratolyl series $X(C_6H_4\text{-}CH_3)_4$ (X = C, Si, Ge, Sn, Pb) were studied by using inelastic neutron scattering to measure the low-energy phonon spectra to directly access the methyl-group torsional modes. The effect of increased molecular radius as a function of the size of the central atom was shown to have direct influence on the methyl dynamics, reinforced with the findings of molecular dynamics and contact surface calculations, based upon the solid-state structures. The torsional modes in the lightest analogue were found to be predominantly intramolecular: the Si and Ge analogues have a high degree of intermolecular methyl–methyl group interactions, whilst the heaviest analogues (Sn and Pb) showed pronounced intermolecular methyl interactions with the whole phonon bath of the lattice modes.

Keywords: crystal engineering · density functional calculations · intermolecular interactions · molecular dynamics · neutron scattering

Introduction

The tetraphenyl derivatives of Group XIV elements have great promise as supramolecular constructs in extended porous networks.[1–3] The tetratolyl Group XIV derivatives are important precursors toward readily usable constructs courtesy of the ease of functionalization at the site of the *para*-methyl group, yet they make a fascinating molecular series in their own right. The methyl groups constitute the very outer contact sphere of individual molecules and so intermolecular interactions potentially dominate the methyl-group dynamics. We have previously shown that the methyl-tunneling spectra of this series, recorded at high-resolution inelastic neutron scattering, vary dramatically across the series.[4] Because the tolyl groups are chemically similar throughout the series, the dominant effect is simply that of molecular size, which is dictated by the central atom. The smallest analogue, tetratolylmethane, $C(C_6H_4\text{–}CH_3)_4$ ($CTol_4$) is, in fact, isostructural with the largest two of the series,[4,5] the stannane and plumbane analogues (all in space group $I\bar{4}$), with the silane and germane species lying in the lower-symmetry space group Pc[6] (Figure 1; CCDC references for all species are: $CTol_4$: 712743, $SiTol_4$: SUCZIZ, $GeTol_4$: SUCZOF, $SnTol_4$: PTOLSN, $PbTol_4$: SOMMEM). The rationale behind this rather bizarre behavior is believed to lie in the contact interactions of the methyl groups on neighboring molecules. Thus, in $CTol_4$, the relatively small molecular radius results in methyl group dynamics independent of those on neighboring molecules. Meanwhile, in $SnTol_4$ and $PbTol_4$, the methyl groups interdigitate with the phenyl groups of nearest neighbor molecules effectively coupling them to the lattice modes. In $SiTol_4$ and $GeTol_4$, the molecular radii are such that the methyl groups on neighboring molecules are potentially in direct contact, resulting in the lowering of symmetry. Whilst the tunneling spectra gave a direct indication of this behavior, we have now sought to directly observe the methyl dynamics in these materials to confirm this simple, yet effective rationale. Because pure torsional modes are inactive in both infrared and Raman spectroscopies due to the absence of a modulation in the dipole moment or polarizability tensor, this requires inelastic scattering of thermally moderated neutrons, for which there are no vibrational selection rules.[7]

[a] Dr. M. C. C. Ng, Dr. J. B. Harper, Prof. J. A. Stride
School of Chemistry, University of New South Wales
Sydney 2052 (Australia)
Fax: (+61) 2-9385-6141
E-mail: j.stride@unsw.edu.au

[b] Dr. A. P. J. Stampfl, Prof. G. J. Kearley, Prof. J. A. Stride
Bragg Institute, Australian Nuclear Science and
Technology Organisation, PMB 1
Menai, NSW 2234 (Australia)

[c] Dr. S. Rols
Institute Laue-Langevin, 6 rue Jules Horowitz
BP156, 38042 Grenoble Cedex 9 (France)

Supporting information for this article is available on the WWW under http://dx.doi.org/10.1002/chem.201202105.

Experimental Section

General: The silane, germane, and stannane compounds were synthesized by using a general reaction Scheme involving the nucleophilic addition of an organometallic reagent to the appropriate tetrachloride (Scheme 1 in the Supporting Information). The synthesis of the carbon analogue proceeded through the corresponding tetraphenyl derivative (Scheme 2 in the Supporting Information) and the plumbane through lead(II) chloride. Single-crystal X-ray datasets were collected for all of the compounds and were found to be consistent with published data, with no phase transitions observed down to $T = 150$ K; X-ray powder-diffraction profiles were

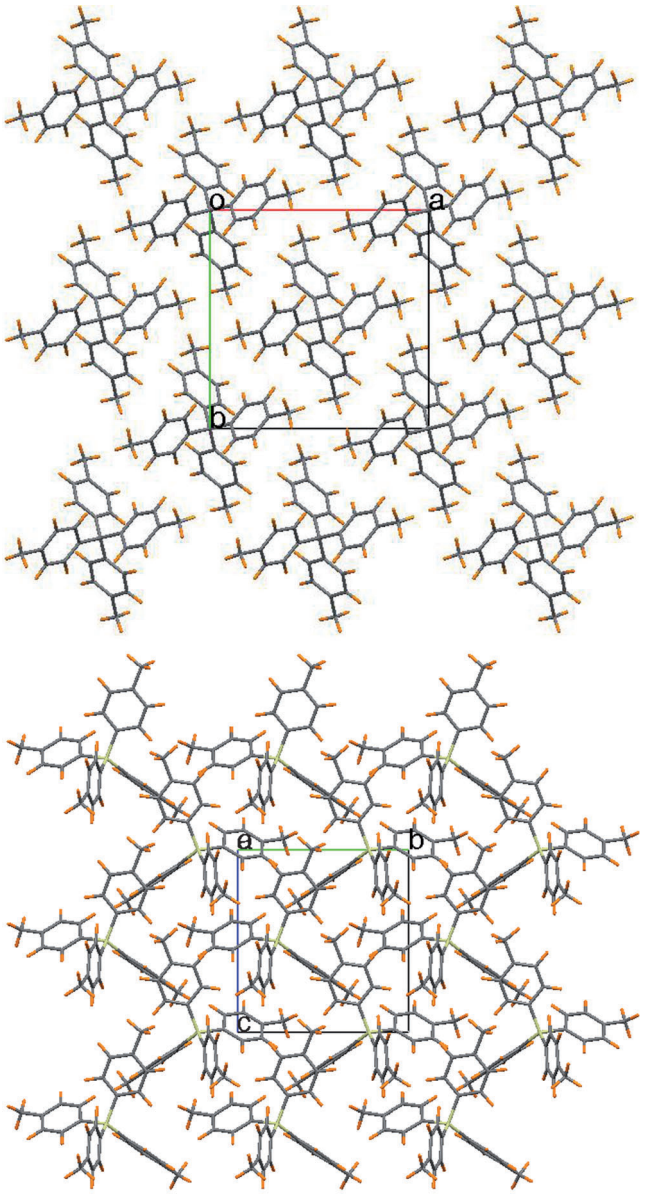

Figure 1. Structure of $CTol_4$ viewed along the *c* axis,[2] isostructural to the Sn (top), and Pb analogues and $SiTol_4$ viewed along the *a* axis,[4] isostructural to $GeTol_4$ (bottom). Carbon atoms: grey, hydrogen atoms: orange, silicon atoms: yellow; note the different methyl group environments.

also collected for all bulk samples and were found to correspond to the calculated profiled based upon the structural data (Scheme 3 in the Supporting Information). Inelastic neutron scattering (INS) data were recorded on two spectrometers, the IN4 time-of-flight spectrometer at ILL, Grenoble, France over a range of temperatures, $2 \leq T \leq 65$ K[8] (all five analogues) and at $T = 10$ K on the triple-axis spectrometer Taipan at the Bragg Institute, ANSTO, Australia ($CTol_4$, $SiTol_4$ and $SnTol_4$).[9]

In the case of the IN4 instrument, the samples were loaded into flat aluminum cans, in such manner that the sample transmission was about 90% (0.1 mm thickness), and loaded into a cryostat prior to irradiation. The instrument was configured for an incident wavelength of 1.52 Å ($E_i = 35.3$ meV). Data were corrected for that of the empty can and were normalized with a vanadium sample to correct for different detector efficiencies and the number of scattering centers in the samples. All data manipulation was performed by using the LAMP program at ILL.[10]

In the case of the Taipan instrument, the samples were loaded into aluminum-foil sachets and mounted onto a cadmium plate, in such manner that data were obtained in reflection, and loaded into a bottom-loading closed-cycle refrigerator. Taipan was configured to a final energy of $E_f = 13.7$ meV at scattering angles 2θ of $40.7° \leq 2\theta \leq 20.0°$ with a range of incident energies $15 \leq E_i \leq 60$ meV, giving a near-linear range of Q between 2.4 and 4.4 Å^{-1}. Data were collected in a stepwise manner and normalized to incident monitor counts.

DFT calculations: A single unit cell was used for the silicon analogue, whilst to obtain a large enough unit to prevent interaction wrap around from the periodic boundaries, a 112 supercell (in unit cell units) was used for the carbon and tin compounds. All DFT calculations were carried out with VASP[12–15] by using the project augmented wave potential[16] (PAW) and the Perdew–Burke–Ernzerhof[17] exchange-correlation functional with the unit cell parameters being constrained to the experimental values. The atomic positions for all cells were optimized by minimizing the forces acting on the atoms by using VASP with high precision: energy cut-off of 500 eV, a convergence condition of 10^{-4} eV, and a $3 \times 3 \times 6$ Monkhorst–Pack *k* point mesh.[18] These minimizations are in excellent agreement with the experimentally determined crystal structures other than slight changes to the methyl-group orientations. These minimized structures were used as the starting point for the MD simulations that were carried out at lower precision with an energy cut-off of 300 eV and a single *k* point. All MD simulations used a time step of 1 fs with a target temperature of 40 K. An initial isokinetic run with velocity scaling of 4 ps was made followed by a thermalization run in the microcanonical ensemble of 8 ps and a production run of 17 ps. Trajectories from the production run were stored for analysis.

Results and Discussion

The datasets from the two instruments are complementary, because they cover different regions of reciprocal space: IN4 accessing a large region of $S(Q,\omega)$ (the scattering law as a function of both momentum transfer, Q and energy transfer, ω), whilst Taipan accessed a cut through $S(Q,\omega)$, but to a higher ω. Both datasets are in full accord with each other and provided vibrational data up to 47 meV (380 cm^{-1}) covering the low-energy lattice modes and large-body reorientations. No significant change in the spectra recorded on IN4 was observed as a function of increased temperature, other than a moderate degree of mode softening and an increased thermal background. The low-temperature spectra for each of the analogues, as was measured on IN4, is shown in Figure 2 and the complementary Taipan data shown in Figure 3.

All of the samples displayed vibrational excitations with a Q dependence characteristic of such modes. The low-energy spectrum of $CTol_4$ is dominated by a single-methyl torsional band, only marginally broader than the instrument resolution, with acoustic phonon branches around 5–10 meV and low-lying molecular deformations between 20 and 30 meV. Despite possessing the same $I\bar{4}$ symmetry, the spectra of the Sn and Pb analogues displayed less pronounced features, with spectral intensity grouped into a broad feature up to approximately 15 meV and a second feature around 20–25 meV. In contrast, the lower symmetry (Pc) of the Si and Ge analogues relates to an apparent splitting of the methyl torsions, consistent with the presence of either nonequivalent, or interacting methyl sites. The Taipan data follows a

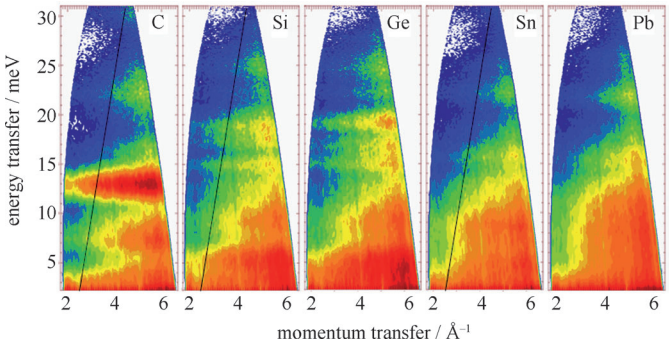

Figure 2. INS spectra of $XTol_4$ (X = C, Si, Ge, Sn, Pb) displayed as recorded on IN4 and displayed as a surface in $S(Q,\omega)$. The false color plots have greater intensity moving from blue to red. The trace superimposed on the C, Si, and Sn spectra represent the trajectory through $S(Q,\omega)$ of the Taipan data.

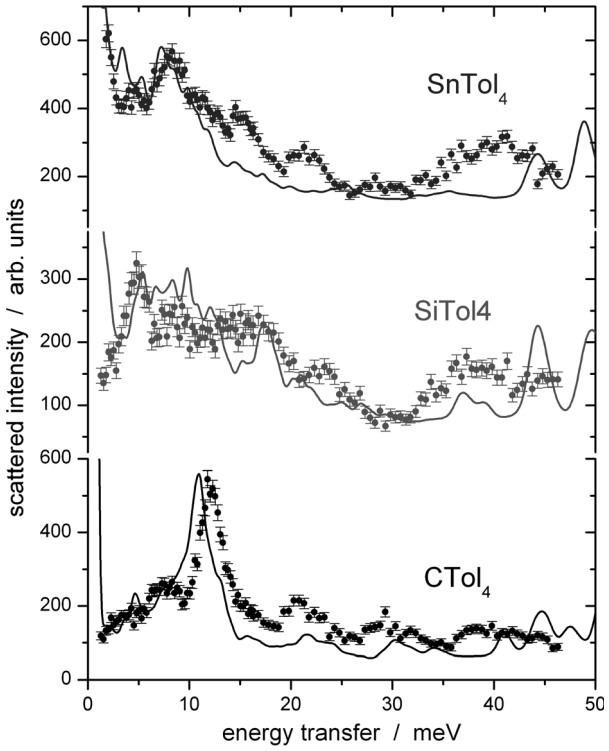

Figure 3. INS spectra obtained on Taipan at 10 K. Spectra correspond to a single, essentially linear path through $S(Q,\omega)$ of $2.4 \le Q \le 4.4$ Å^{-1} corresponding to $1.3 \le \omega \le 26.3$ meV. Data points correspond to recorded spectra and solid lines correspond to calculated spectral functions scaled only in intensity, with no least-squares fitting to the data.

given trajectory through $S(Q,\omega)$, which was found to be fully consistent with that obtained on IN4. This general picture of the methyl-torsional dynamics is in full accord with both the crystalline structures and the high-resolution methyl-tunneling spectra reported previously.[4]

By summing across the whole of the measured $S(Q,\omega)$ surface, a vibrational density of states across the accessible regions of the Brillouin zone was obtained (Figure 4). Again, this representation highlights the fact that discrete molecular excitations become less pronounced in moving

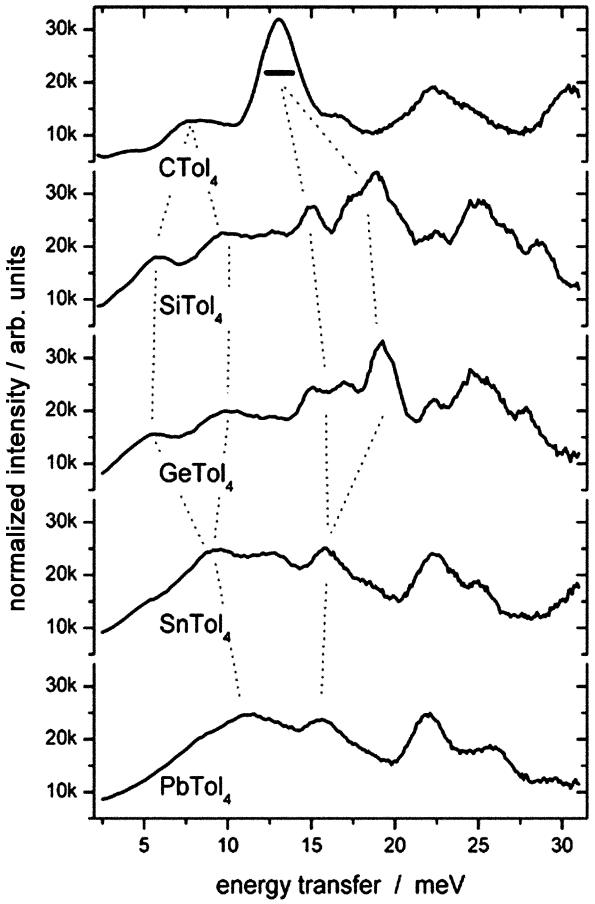

Figure 4. Low-energy INS spectra across the $XTol_4$ series from $CTol_4$ (top) to $PbTol_4$ (bottom) obtained at $T = 1.5$ K. The methyl torsions lie in the region of 10–20 meV; dotted lines represent the symmetry splitting of the methyl torsions. Spectral resolution is indicated by solid black line superimposed onto the $CTol_4$ spectrum.

from $CTol_4$ down to $PbTol_4$, despite the symmetry associated considerations. The rational explanation for this behavior is that the symmetry allowed phonon spectrum becomes more extensive, when the central atom increases in size when moving through the $I\bar{4}$ isostructural compounds $CTol_4$, $SnTol_4$, and $PbTol_4$. In the case of the C analogue, the methyl groups undergo largely unimolecular methyl torsions, which are then increasingly mixed into the phonon spectrum, when the central atom effectively exerts intermolecular pressure, resulting in a dispersive behavior. This results in the systematic decrease of the spectral intensity of the peak assigned to be predominantly due to pure-methyl torsions (an approximation, which is evidently less valid upon descending Group XIV) to give relative intensities of 7.67:1.31:1 for the C, Sn, and Pb analogues, respectively. For the particular case of incoherent neutron scattering in the one-phonon approximation, the intensity I can be represented as follows:[11]

$$I \propto S_{inc}(Q,\omega) \propto \sigma Q^2 \exp\left(-\frac{Q^2\langle u^2\rangle}{3}\right)\frac{n(\omega)+1}{\omega}g(\omega)$$

in which σ is the total neutron-scattering cross-section of the molecule, $n(\omega)$ is the Bose occupation factor, and $<u(T)^2>$ is the mean-square displacement of the atoms, and $g(\omega)$ is the density of states. The incoherent cross-section of protons is 80.26×10^{-24} cm^2, which is around an order of magnitude larger than any other cross-section in the samples studied. Therefore, the recorded spectra are heavily proton weighted, and so only proton motions need be considered in $g(\omega)$ to a first approximation. When all of the IN4 spectra were normalized for the molar concentration (the effective number of scattering centers), the partial cross-sections of the methyl groups were equal in each spectrum, causing the final intensity of the methyl torsions to be proportional to the mean-square displacement $<u(T)^2>$ of the protons undergoing the methyl torsion. Therefore, the relative amplitudes of motion in $CTol_4$, $SnTol_4$, and $PbTol_4$ are 2.76:1.15:1.0, respectively. This picture of increasingly restricted motion is consistent with the methyl groups in $CTol_4$ being relatively sterically unhindered, whilst in $SnTol_4$ and $PbTol_4$, the methyl groups are increasingly hindered due to the interdigitation into the pockets between the aromatic groups of neighboring molecules, resulting in greater mixing with the general-phonon spectrum. In contrast, the methyl-torsional amplitudes in $SiTol_4$ and $GeTol_4$ are essentially the same, and both are similar to that in $CTol_4$; however, this intensity is distributed over the symmetry-split modes.

To evaluate the notion of increasingly hindered Me groups upon descending Group XIV beyond the single-phonon approximation, detailed molecular dynamics were performed for the C, Si and Sn analogues. The interactions of interest in the present study are comparatively short range, so that to avoid the uncertainties of empirical force-field methods, DFT methods were used to calculate the energies (see the Experimental Section).

The main validation of the MD simulations is their ability to reproduce the recorded INS spectra, which were obtained by using the program nMoldyn.[19] The measured dynamical structure factor $S(Q,\omega)$ is related to the simulated trajectories through a Fourier transform of the incoherent intermediate scattering function:

$$F(Q,t) = \sum b_i \langle \exp[-iQ\cdot R_i(0)]\exp[iQ\cdot R_i(t)]\rangle$$

in which the momentum transfer Q and time t are on a regular grid, $R(0)$ is the atomic position at $t=0$, and b is the total scattering cross-section (in the incoherent approximation). The summation was done over all atoms (i), but it approximates to a sum over only the hydrogen atoms due to the very large incoherent cross section of H. A comparison of the calculated spectra of the analogues with the spectra recorded on Taipan and IN4 (Figures 3 and 5, respectively) shows reasonable agreement, and is certainly adequate for an assignment of the regions of spectral intensity.

Our major interest is in the dynamics of the methyl groups and the aromatic rings to which they are attached. They are easily separated by calculating the separate frequency spectra of the methyl and aromatic protons. Whilst the motion of the Me protons will be principally a convolution of the methyl-group torsions with torsions of the aromatic ring, the ring protons will only have the latter motion. These frequency spectra (intensity was transformed to be INS spectra) are illustrated in Figure 5. In the case of the C and Si analogues, the total spectrum is dominated by the motion of the Me groups, with only marginal contribution from the ring hydrogen atoms. However, this distinction is not as apparent in the case of the Sn compound, in which

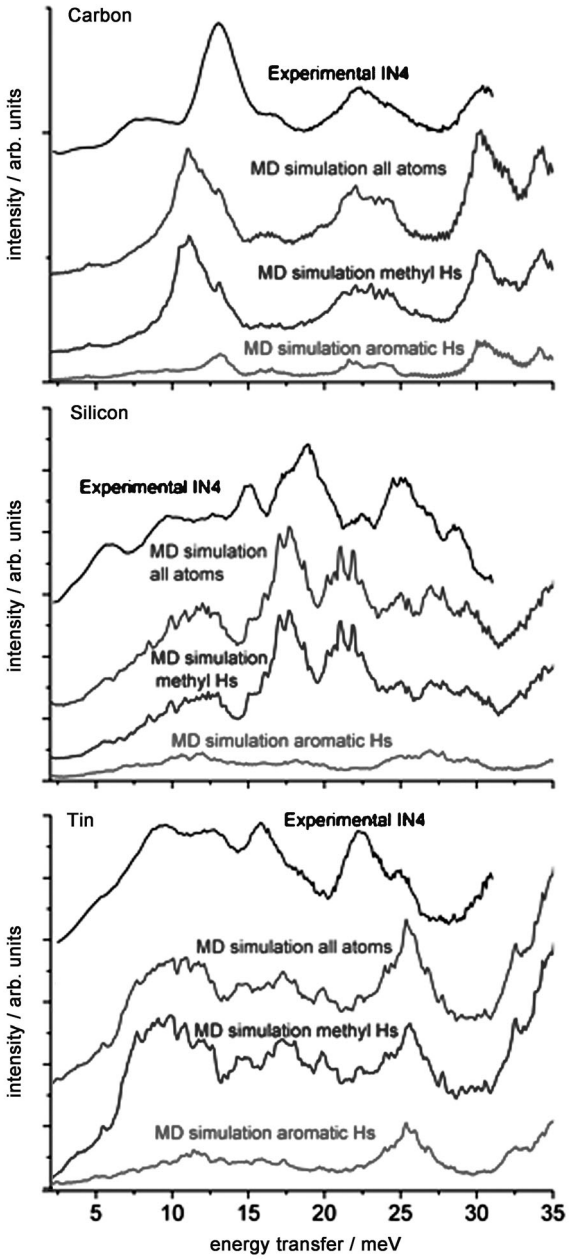

Figure 5. Comparison of recorded and calculated spectra for $XTol_4$ (X = C, Si, Sn). Calculated spectra are shown for all atoms (complete spectrum) and partial spectra— only for Me group and only aromatic-group hydrogen atoms.

the Me and ring hydrogen atoms both make considerable contributions to the total spectrum, consistent with the picture of increased mode mixing in the larger analogues. As a final verification of this model, the low-energy phonon spectrum can be approximated to the Fourier transform of the autocorrelation function of the whole body motions of the molecules within the boundary confines of the molecular dynamics simulation (Figure 6). Whilst the molecular motions

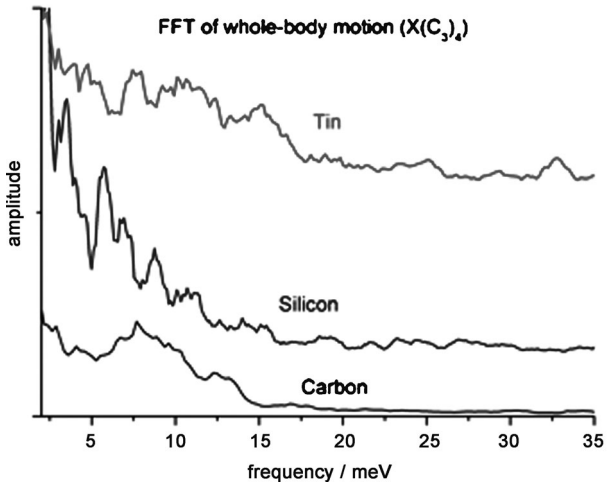

Figure 6. Fast Fourier transform of the autocorrelation function of whole-body motions for $XTol_4$ (X = C, Si, Sn).

of the C and Si analogues are largely separated from the respective Me group dynamics, this is not the case for the Sn system, representing a considerable mode mixing between the Me motions and the molecular-phonon spectrum in the latter.

The degree of mode mixing induced by nearest-neighbor interactions can be assessed by investigating the Hirshfeld molecular surfaces calculated from the solid-state structures, effectively the contact surfaces of discrete molecules.[20] By using the freely available CrystalExplorer package,[21] the Hirshfeld surfaces of the $XTol_4$ molecules were investigated based upon their published X-ray structures with hydrogen atoms added in riding positions. Figure 7 shows the value d_{norm} mapped onto the surface for each analogue: d_{norm} normalizes the interatomic separation for the corresponding van der Waals interactions, and as such, negative values (shown in red) have interatomic separations below the van der Waals contact distance, whilst blue regions on the surface have positive d_{norm} values, or separations greater than the corresponding van der Waals radii. As such, white regions mapped onto the Hirshfeld surface represent near van der Waals interactions, which can be seen to generally increase moving down the group from the C to Pb analogues. In $CTol_4$, the closest interactions are intermolecular H···C interactions and H···H contacts at the ring (Ar) sites. Moving to the lower symmetry Si and Ge analogues, the prominent (below van der Waals) interactions are dominated by intermolecular Me interactions, with additional inter-

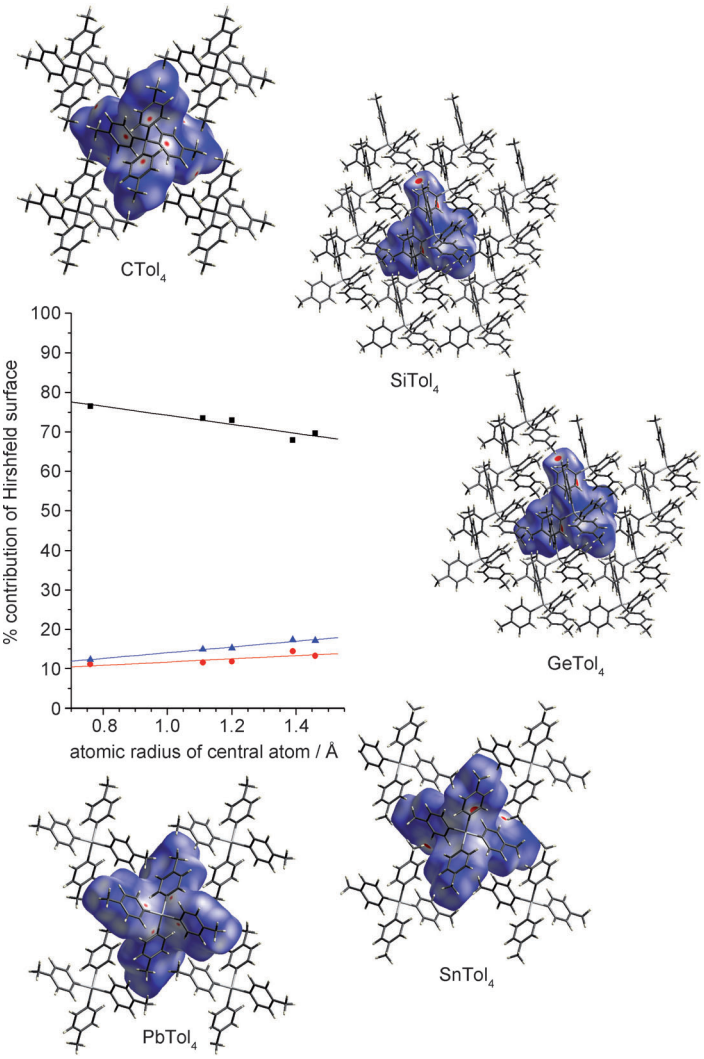

Figure 7. Hirshfeld surfaces mapped with effective van der Waals interactions (d_{norm}; red ⟨van der Waals; blue⟩ van der Waals) for $XTol_4$ (X = C, Si, Ge, Sn, Pb). Inset: dependence of nearest-neighbor contact types with the size of the central atom. ■ = H(i)···H(e); ▲ = C(i)···H(e); ● = H(i)···C(e).

molecular H···C contacts. Back to the high-symmetry Sn and Pb analogues and the Me interactions are more coupled to the general phonon bath, with hot spots corresponding to intermolecular Me–C and H(Ar)···C contacts in $SnTol_4$ and only the H(Ar)···C contacts in $PbTol_4$, although the regions of near van der Waals interactions are more pronounced throughout the whole of the surfaces. Further analysis of these surfaces provides insights to the different types of interactions according a % contribution to the complete surface: in this way, atoms inside the Hirshfeld surface, X(i), can be correlated to atoms external to the surface, X(e), providing a greater impression of the overall contact terms.[22] Generally, H···H interactions decrease as the central atom increases in size, with a corresponding increase in C···H interactions, when the whole structure becomes more interdigitated. Indeed, a plot of the relative contributions of H(i)···H(e), C(i)···H(e), and H(i)···C(e) display a linear re-

sponse to the central-atom size, underlining the size effect of X in these materials.

Finally, the present work based upon the direct observation of the methyl torsions, MD simulations, and near-neighbor contacts across the whole series is fully consistent with our previously published work into the methyl-tunneling spectra.[4] The tunneling spectra are uniquely sensitive to the methyl-group environment,[23] and the tunneling spectra of the $XTol_4$ compounds highlighted that the methyl groups became increasingly hindered moving down the Group.[4] However, now we have the complete picture with both the tunneling and torsional frequencies, which allows to accurately evaluate the local rotational potential and to compare that to the time-averaged contact surfaces based upon the crystallographic data. The rotational potential of a rigid methyl-group rotor hindered by a potential barrier V, when it precesses through an angle ϕ, and can be expressed by the Hamiltonian:[24]

$$H = \frac{-\hbar^2}{2I}\frac{\delta^2}{\delta\phi^2} + V$$

in which the potential I is the moment of inertia of the rotor, and V can be represented as a Fourier expansion:

$$V = \sum_{n\geq 1}\frac{1}{2}V_{3n}\{1+\cos[3n(\phi+f_{3n})]\}$$

in which only the first two terms, $n=1$ and 2 (V_3 and V_6), are considered (with a relative phase of $f=f_6-f_3$), allowing the definition of the potential-energy trajectory, based on tunneling frequencies, which can then be directly related to the torsional modes (Table 1). The $CTol_4$ tunneling spectra gave three distinct frequencies at 4.99(3), 6.87(31), and 8.52(24) μeV, which correspond to calculated first torsional modes at 12.8, 12.1, and 11.8 meV, respectively (and a second torsion at 22 meV), with threefold potential energy barriers of 33, 35.5, and 31.0 meV. Likewise, the estimated tunneling frequency of $SnTol_4$ of 0.6 μeV suggests a first torsional frequency of 16 meV and a second at 30 meV, with a threefold potential with a barrier height of 55 meV. Finally, the tunneling spectrum of SiTol4 with a mode at 2.82(1) μeV can only be rationalized with the observed torsional spectrum in a sixfold potential having a barrier height of 24.5 meV, giving torsions at 20.5 and 23 meV. This picture, purely based on the observed spectral modes, only obtainable in a combination of neutron-scattering experiments, is fully consistent with the crystallographic data and calculated Hirshfeld surfaces; isolated rotors in $CTol_4$, interacting rotors in $SiTol_4$ and $GeTol_4$, and rotors more generally coupled into the phonon bath in $SnTol_4$ and $PbTol_4$ as a result of interdigitation between neighboring molecules.

Table 1. Calculated torsional frequencies based on the measured tunneling modes Ref [4] and are directly comparable to the inelastic neutron-scattering spectra.[a]

	Tunneling frequency [μeV]	Calculated torsional frequency [meV]		Barrier height [meV]	Rotational potential
$CTol_4$	4.99	12.8	22	33	threefold
	6.57	12.1	22	35.5	
	8.53	11.8	22	31.0	
$SiTol_4$	2.82	13.7	23	40.5	threefold
		20.5		24.5	sixfold
$SnTol_4$	0.6	16	30	55	threefold

[a] $XTol_4$ species within the $I\bar{4}$ space group are best described with threefold potentials, whilst those in Pc have sixfold potentials consistent with interacting rotors (shaded threefold potential for $SiTol_4$ highlights a poor correlation to observation).

Conclusion

The Me motions in the series of compounds $XTol_4$ (X = C, Si, Ge, Sn, Pb) are hindered by the effects of molecular packing when the central atom size increases, resulted in an initial increase in the mean vibrational frequency and finally resulted in strongly perturbed methyls by virtue the restricted amplitude of vibration, making the series an ideal-case study for the confinement of diffusive motions. The characteristic behavior of the Me groups upon central-atom substitution are fully in accord with both the crystallographic and spectroscopic data and is clearly rationalized with the concept of increased molecular crowding or chemical pressure; reinforced with detailed molecular dynamics simulations and numerical modeling of the molecular contact surfaces, which highlight nearest-neighbor contacts.

Acknowledgements

This research was supported by UNSW ECR and ARC (DP0880199) grants and an AMFRP access grant (No. 07/08-N-16).

[1] a) D. Laliberté, T. Maris, J. D. Wuest, *Can. J. Chem.* **2004**, *82*, 386–398; b) H. M. El-Kaderi, J. R. Hunt, J. L. Mendoza-Cotés, A. P. Côté, R. E. Taylor, M. O'Keeffe, O. M. Yaghi, *Science* **2007**, *316*, 268–272.
[2] W. Lu, D. Yuan, D. Zhao, C. I. Schilling, O. Plietzsch, T. Muller, S. Bräse, J. Guenther, J. Blümel, R. Krishna, Z. Li, H.-C. Zhou, *Chem. Mater.* **2010**, *22*, 5964–5972.
[3] A. Trewin, A. I. Cooper, *Angew. Chem.* **2010**, *122*, 1575–1577; *Angew. Chem. Int. Ed.* **2010**, *49*, 1533–1535.
[4] M. C. C. Ng, D. J. Craig, J. B. Harper, L. van-Eijck, J. A. Stride, *Chem. Eur. J.* **2009**, *15*, 6569–6572.
[5] M. Charissé, S. Roller, M. Dräger, *J. Organomet. Chem.* **1992**, *427*, 23–31.
[6] C. Schneider, M. Dräger, *J. Organomet. Chem.* **1991**, *415*, 349–362.
[7] P. C. H. Mitchell, S. F. Parker, A. J. Ramirez-Cuesta, *Vibrational Spectroscopy with Neutrons: With applications in Chemistry, Biology, Materials Science and Catalysis*, World Scientific Publishing, London, **2005**.
[8] a) http://www.ill.fr/YellowBook/IN4/; b) G. Cicognani, H. Mutka, F. Sacchetti, *Physica B* **2000**, *276–278*, 83–84.
[9] S. Danilkin, G. Horton, R. Moore, G. Braoudakis, M. Hagen, *J. of Neutron Research* **2007**, *15*, 55–60.
[10] LAMP, the Large Array Manipulation Program, http://wwwold.ill.fr/data_treat/lamp/lamp.html.

[11] S. W. Lovesey, *Theory of Neutron Scattering from Condensed Matter*, Clarendon, Oxford, **1984**.
[12] G. Kresse, J. Furthmuller, *Phys. Rev. B* **1996**, *54*, 11169–11186.
[13] G. Kresse, J. Furthmuller, *Comput. Mater. Sci.* **1996**, *6*, 15–50.
[14] G. Kresse, J. Hafner, *Phys. Rev. B* **1993**, *47*, 558–561.
[15] G. Kresse, D. Joubert, *Phys. Rev. B* **1999**, *59*, 1758–1775.
[16] P. E. Blöchl, *Phys. Rev. B* **1994**, *50*, 17953–17979.
[17] J. P. Perdew, K. Burke, M. Ernzerhof, *Phys. Rev. Lett.* **1996**, *77*, 3865–3868.
[18] H. J. Monkhorst, J. D. Pack, *Phys. Rev. B* **1976**, *13*, 5188–5192.
[19] G. R. Kneller, V. Keiner, M. Kneller, M. Schiller, *Comp. Phys. Commun.* **1995**, *91*, 191–214.
[20] M. A. Spackman, D. Jayatilaka, *CrystEngComm* **2009**, *11*, 19–32.
[21] http://ra.bcs.uwa.edu.au/CrystalExplorer/wiki/index.php/Main_Page.
[22] J. J. McKinnon, D. Jayatilaka, M. A. Spackman, *Chem. Commun.* **2007**, 3814–3816.
[23] B. Nicolaï, G. J. Kearley, M. R. Johnson, F. Fillaux, E. Suard, *J. Chem. Phys.* **1998**, *109*, 9062–9074.
[24] M. R. Johnson, B. Frick, H. P. Trommsdorff, *Chem. Phys. Lett.* **1996**, *258*, 187–193.

Received: June 14, 2012
Published online: ■■ ▮▮, 0000

Crystal Engineering

*M. C. C. Ng, J. B. Harper, A. P. J. Stampfl, G. J. Kearley, S. Rols, J. A. Stride** ..... ▮▮▮▮–▮▮▮▮

Central-Atom Size Effects on the Methyl Torsions of Group XIV Tetratolyls

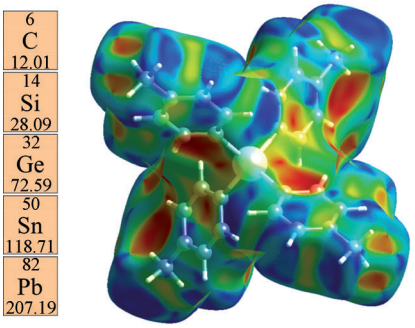

Size matters! The size of the central atom in the Group XIV tetratolyls was shown to determine the solid-state structures courtesy of the effect that it has on the overall size of the molecules (see figure). Because the outer-most methyl groups enter into close intermolecular interactions (for the Si and Ge analogues), the structure is driven to lower symmetry; as a consequence, the smallest (C) and largest (Sn and Pb) analogues are isostructural.

